Journal of Microbiology (2022) Vol. 60, No. 12, pp. 1139–1152
DOI 10.1007/s12275-022-2347-x
eISSN 1976-3794
pISSN 1225-8873

Negative regulation of the *acsA1* gene encoding the major acetyl-CoA synthetase by cAMP receptor protein in *Mycobacterium smegmatis*

Eon-Min Ko[1#], Yuna Oh[1], and Jeong-Il Oh[1,2*]

[1]*Department of Integrated Biological Science, Pusan National University, Busan 46241, Republic of Korea*
[2]*Microbiological Resource Research Institute, Pusan National University, Busan 46241, Republic of Korea*
[#]*Present address: Division of Bacterial Disease Research, Center for Infectious Disease Research, National Institute of Infectious Diseases, National Institute of Health, Korea Disease Control and Prevention Agency, Osong 28159, Republic of Korea*

(Received Aug 4, 2022 / Revised Sep 23, 2022 / Accepted Sep 23, 2022)

Acetyl-CoA synthetase (ACS) is the enzyme that irreversibly catalyzes the synthesis of acetyl-CoA from acetate, CoA-SH, and ATP via acetyl-AMP as an intermediate. In this study, we demonstrated that AcsA1 (MSMEG_6179) is the predominantly expressed ACS among four ACSs (MSMEG_6179, MSMEG_0718, MSMEG_3986, and MSMEG_5650) found in *Mycobacterium smegmatis* and that a deletion mutation of *acsA1* in *M. smegmatis* led to its compromised growth on acetate as the sole carbon source. Expression of *acsA1* was demonstrated to be induced during growth on acetate as the sole carbon source. The *acsA1* gene was shown to be negatively regulated by Crp1 (MSMEG_6189) that is the major cAMP receptor protein (CRP) in *M. smegmatis*. Using DNase I footprinting analysis and site-directed mutagenesis, a CRP-binding site (GGTGA-N_6-TCACA) was identified in the upstream regulatory region of *acsA1*, which is important for repression of *acsA1* expression. We also demonstrated that inhibition of the respiratory electron transport chain by inactivation of the major terminal oxidase, aa_3 cytochrome *c* oxidase, led to a decrease in *acsA1* expression probably through the activation of CRP. In conclusion, AcsA1 is the major ACS in *M. smegmatis* and its gene is under the negative regulation of Crp1, which contributes to some extent to the induction of *acsA1* expression under acetate conditions. The growth of *M. smegmatis* is severely impaired on acetate as the sole carbon source under respiration-inhibitory conditions.

Keywords: acetate, acetyl-CoA synthetase, cAMP-receptor protein, gene regulation, *Mycobacterium smegmatis*

Introduction

The survival and fitness of bacteria in a given environment rely on their ability to utilize available nutrients efficiently. *Mycobacterium tuberculosis*, the causative agent of tuberculosis, is an intracellular pathogen that resides and replicates within host macrophages. During infection, host-derived fatty acids and cholesterol have been suggested to be important carbon and energy sources for *M. tuberculosis* (Bloch and Segal, 1956; Pandey and Sassetti, 2008; Lee *et al.*, 2013; VanderVen *et al.*, 2015). Intriguingly, acetate was found in tissue extracts, and acetate accumulation has been detected in the lung of guinea pigs infected with *M. tuberculosis* (Somashekar *et al.*, 2011). Mycobacteria including *M. tuberculosis* are capable of using acetate as the sole carbon source *in vitro* (Shin *et al.*, 2011; Masiewicz *et al.*, 2012; Puckett *et al.*, 2017). Therefore, it has been suggested that acetate could be also a potential carbon source during infection (Munoz-Elias and McKinney, 2005; Pandey and Sassetti, 2008; Beste *et al.*, 2013).

Assimilation of acetate is initiated by acetate activation, the process that converts acetate to acetyl-CoA. Acetate activation is accomplished by two separate pathways, the pathway comprising two sequential reactions catalyzed by acetate kinase (ACK) and phosphotransacetylase (PTA) and the single-reaction pathway catalyzed by acetyl-CoA synthetase (ACS) (Wolfe, 2005). In the ACK-PTA pathway, ACK catalyzes the reaction that converts acetate to acetyl phosphate using ATP as a phosphate donor, and the resulting acetyl phosphate is subsequently converted to acetyl-CoA by PTA (Reinscheid *et al.*, 1999; Wolfe, 2005). During growth on excess glycolytic or acetyl-CoA-producing substrates including glucose, pyruvate, and fatty acids, as well as under TCA cycle-inhibitory conditions, the ACK-PTA pathway operates reversely to avoid the accumulation of acetyl-CoA in the cell (Brown *et al.*, 1977; Sadykov *et al.*, 2013; Enjalbert *et al.*, 2017), which indicates the ACK-PTA pathway not only functions in acetate assimilation, but also in acetate production (Kumari *et al.*, 1995; Enjalbert *et al.*, 2017). ACS irreversibly catalyzes the synthesis of acetyl-CoA from acetate, CoA-SH, and ATP via acetyl-AMP as an intermediate (Berg, 1956; Webster, 1963; Wolfe, 2005). ACS is a member of the acyl-AMP-forming enzyme superfamily (Van den Berg and Steensma, 1995; Wolfe, 2005; Kuprat *et al.*, 2020). The Km value of ACS for acetate is lower than that of ACK (Fox and Roseman, 1986; Kumari *et al.*, 1995; Wolfe, 2005). Therefore, when the concentration of acetate is low in the environment, acetate assimilation is assumed to occur preferentially by the high-affinity ACS pathway. Mycobacteria possess functional ACS enzymes that generate acetyl-CoA from acetate (Li *et al.*, 2011; Rücker *et al.*, 2015; Liu *et al.*, 2018). Similar to other bacterial ACSs, the mycobacterial ACSs can also convert propionate to propionyl-CoA (Li *et al.*, 2011; Liu *et al.*, 2018).

The regulation of the gene encoding ACS at the transcrip-

*For correspondence. E-mail: joh@pusan.ac.kr; Tel.: +82-51-510-2593; Fax: +82-51-514-1778

tional level has been studied extensively in several bacteria. In *Escherichia coli*, expression of *acs* is upregulated during entry into the stationary phase and in the presence of acetate, and the induction of *acs* expression is controlled in response to changes in intracellular levels of cAMP by a global transcriptional regulator, CRP (cAMP receptor protein) (Kumari *et al.*, 2000; Beatty *et al.*, 2003). The involvement of FIS (factor for inversion stimulation) and IHF (integration host factor) in negative regulation of *acs* expression has been also demonstrated in *E. coli* (Browning *et al.*, 2004). Furthermore, expression of *acs* has been demonstrated to be positively regulated by FNR (fumarate and nitrate reductase regulator) in *E. coli* (Kumari *et al.*, 2000). Since FNR is an oxygen-responsive transcriptional regulator, it has been suggested that *acs* expression is regulated in response to changes in oxygen tensions (Kumari *et al.*, 2000; Clark and Cronan, 2005). In *Bacillus subtilis*, expression of *acs* is controlled by CcpA (catabolite control protein A) and the GTP-sensing transcriptional regulator CodY in response to carbon availability (Grundy *et al.*, 1994; Zalieckas *et al.*, 1998; Molle *et al.*, 2003). In mycobacteria, expression of *acs* has been demonstrated to be induced during growth on acetate as the sole carbon source, and disruption of the *acs* gene has been shown to impair growth on acetate as the sole carbon source (Hayden *et al.*, 2013; Chopra *et al.*, 2014; Rücker *et al.*, 2015; Liu *et al.*, 2018). It was recently reported that expression of *acs* is positively regulated by the nitrogen-sensing regulator GlnR in response to changes in nitrogen levels in *Mycobacterium smegmatis* (Liu *et al.*, 2018).

Protein acetylation at lysine residues is an important regu-

Table 1. Strains and plasmids used in this study

Strain/plasmid	Relevant phenotype/genotype	References
Strains		
E. coli DH5α	Φ80d*lacZ*ΔM15 Δ*lacU169 recA1 endA1 hsdR17 supE44 thi1 gyrA96 relA1*	Jessee (1986)
E. coli BL21 (DE3)	F$^-$, *ompT hsdS*$_B$ (r_B^-, m_B^-) *dcm gal* λ (DE3)	Promega
M. smegmatis Δ*crp1*	*MSMEG_6189* (*crp1*) insertion mutant derived from *M. smegmatis* mc^{2}155; Hyg^r	Lee *et al.* (2014)
M. smegmatis Δ*crp2*	*MSMEG_0539* (*crp2*) deletion mutant derived from *M. smegmatis* mc^{2}155	Ko and Oh (2020)
M. smegmatis Δ*pta*	*MSMEG_0783* (*pta*) deletion mutant derived from *M. smegmatis* mc^{2}155	This study
M. smegmatis Δ*ackA*	*MSMEG_0784* (*ackA*) deletion mutant derived from *M. smegmatis* mc^{2}155	This study
M. smegmatis Δ*acsA1*	*MSMEG_6179* (*acsA1*) deletion mutant derived from *M. smegmatis* mc^{2}155	This study
M. smegmatis Δ*glnR*	*MSMEG_5784* (*glnR*) deletion mutant derived from *M. smegmatis* mc^{2}155	This study
M. smegmatis Δ*ramA*	*MSMEG_5651* (*ramA*) deletion mutant derived from *M. smegmatis* mc^{2}155	Ko *et al.* (2021)
M. smegmatis Δ*ramB*	*MSMEG_0906* (*ramB*) deletion mutant derived from *M. smegmatis* mc^{2}155	Ko *et al.* (2021)
M. smegmatis Δaa_3	*MSMEG_4268* (*ctaC*) deletion mutant derived from *M. smegmatis* mc^{2}155	Jeong *et al.* (2018)
Plasmids		
pKOTs	Hyg^r; pKO-based vector constructed by inserting the HindIII-KpnI fragment containing pAL500Ts and pUC ori derived from pDE	Jeong *et al.* (2013)
pEMII	Km^r; promoterless *lacZ*	Ko *et al.* (2021)
pUC19	Amp^r; *lacPOZ'*	Yanisch-Perron *et al.* (1985)
pT7-7	Amp^r; T7 promoter, ribosome binding site, and translation start codon overlapping with NdeI site	Tabor and Richardson (1985)
pMV306	Km^r; integration vector containing int and the attP site of mycobacteriophage L5 for integration into the mycobacterial genome	Stover *et al.* (1991)
pBluescript II KS+	Amp^r; *lacPOZ'*	Stratagene
pUC19acsA1FootR	pUC19::0.278-kb EcoRI-HindIII fragment containing the *acsA1* promoter region	This study
pUC19pta	pUC19::2.305-kb EcoRI-HindIII fragment containing the *pta*	This study
pUC19Δpta	pUC19::0.940-kb EcoRI-HindIII fragment containing 1.365 kb-deleted *pta*	This study
pKOTsΔpta	pKOTs::0.945-kb EcoRV-HindIII fragment containing Δ*pta*	This study
pKOTsΔackA	pKOTs::0.909-kb EcoRV-HindIII fragment containing Δ*ackA*	This study
pKOTsΔacsA1	pKOTs::0.804-kb EcoRV-HindIII fragment containing Δ*acsA1*	This study
pKOTsΔglnR	pKOTs::0.880b EcoRV-HindIII fragment containing Δ*glnR*	This study
pEMIIacsA1	pEMII:: 0.437-kb ClaI-XbaI fragment containing the *acsA1* promoter region	This study
pBSIIacsA1	pBluescript II KS+:: 0.437-kb ClaI-XbaI fragment containing the *acsA1* promoter region	This study
pBSIIacsA1M	pBSIIacsA1 with two point mutations (AC→GT) in CBS	This study
pEMIIacsA1M	pEMII:: 0.437-kb ClaI-XbaI fragment from pBSIIacsA1M	This study
pEMIIicl1	pEMII:: 0.542-kb ClaI-XbaI fragment containing the *icl1* promoter region	Ko *et al.* (2021)
pT7-7Crp	pT7-7::0.693-kb NdeI-HindIII fragment containing *crp1* (*MSMEG_6189*) with 6 His codons before its stop codon	Bong *et al.* (2019)
pT7-7Crp2	pT7-7::0.693-kb NdeI-HindIII fragment containing *crp2* (*MSMEG_0539*) with 6 His codons before its stop codon	This study
pMV306crp	pMV306::1.239-kb ClaI-HindIII fragment containing *crp1*	Lee *et al.* (2014)
pMV306acsA1	pMV306::2.588-kb XbaI-HindIII fragment containing *acsA1*	This study
pMV306ctaC	pMV306::1.37-kb XbaI-HindIII fragment containing *ctaC*	Jeong *et al.* (2018)

*Abbreviations: Amp^r, ampicillin resistance; Hyg^r, hygromycin resistance; Km^r, kanamycin resistance.

latory mechanism that reversibly modulates the activity of ACS post-translationally. Acetylation of ACS by protein lysine acetyltransferase (PAT) has been shown to inhibit the enzyme activity (Starai and Escalante-Semerena, 2004; Gardner *et al.*, 2006; Yu *et al.*, 2008; Crosby *et al.*, 2010). Deacetylation of acetylated ACS has been shown to lead to reactivation of the ACS activity. The deacetylation reaction is catalyzed by the NAD^+-dependent deacetylase CobB in *Salmonella enterica* and AcuC and SrtN in *B. subtilis* (Starai *et al.*, 2002; Gardner and Escalante-Semerena, 2009). In mycobacteria, PAT acetylates ACS in a cAMP-dependent manner, and the sirtuin-like deacetylase SrtN deacetylates ACS using NAD^+ (Gu *et al.*, 2009; Xu *et al.*, 2011; Lee *et al.*, 2012; Hayden *et al.*, 2013; Nambi *et al.*, 2013).

cAMP is a universal secondary messenger and used for intracellular signal transduction in bacteria, fungi, and complex eukaryotes. Fluctuations in cAMP levels modulate downstream regulatory effects through allosteric binding to cAMP-binding proteins such as CRP and PAT. The CRP proteins are global transcription factors with a quaternary structure of homodimer. They are involved in the regulation of expression of many genes that are implicated in diverse metabolic and cellular processes in prokaryotes, including carbon utilization, respiration, virulence, reactivation of non-replicating dormant cells, and stress responses, etc (Utsumi *et al.*, 1989; Rickman *et al.*, 2005; Shimada *et al.*, 2011; Aung *et al.*, 2014; Green *et al.*, 2014; Heroven and Dersch, 2014). Unlike *M. tuberculosis* with a single CRP, *M. smegmatis* has two genes (*MSMEG_6189*, *crp1*; *MSMEG_0539*, *crp2*) encoding CRP. Crp1 shares 78% sequence identity with Crp2 at the amino acid level (Sharma *et al.*, 2014; Aung *et al.*, 2015). Although Crp1 and Crp2 have been demonstrated to possess different biochemical properties such as their binding affinity for cAMP and cAMP-induced changes in DNA-binding affinity (Sharma *et al.*, 2014; Aung *et al.*, 2015), the close similarity in the sequences of their helix-turn-helix (HTH) domains suggests that the two proteins are likely to recognize similar DNA-binding sequences (Sharma *et al.*, 2014). Recently, Crp1 has been demonstrated to be the major CRP in *M. smegmatis*, and the failure of obtaining a *crp1crp2* double knockout mutant allowed us to suggest that CRP might be indispensable for survival or growth of *M. smegmatis* (Ko and Oh, 2020).

In this study, we revealed that AcsA1 (MSMEG_6179) is the major ACS among four ACSs found in *M. smegmatis*. Expression of *acsA1* was demonstrated to be induced during growth of *M. smegmatis* on acetate as the sole carbon source. The *acsA1* gene was shown to be under the negative regulation of CRP. We also demonstrated that inhibition of the respiratory electron transport chain (ETC) by inactivation of the major terminal oxidase, aa_3 cytochrome *c* oxidase, led to a decrease in *acsA1* expression probably through the activation of CRP.

Table 2. Oligonucleotides used in this study

Oligonucleotide	Nucleotide sequences (5′→3′)	Purpose
F_acsA1lacZ	ATATTCTAGACCGACAGTTGCACCGCA	*acsA1*::*lacZ* fusion
R_acsA1lacZ	ATATATCGATGGCCTCGGCGTACAACTC	*acsA1*::*lacZ* fusion
F_acsA1_M	TTCGGTGACTAGGCTCGTAGCCATGTCGAACCC	Site-directed mutagenesis
R_acsA1_M	GGGTTCGACATGGCTACGAGCCTAGTCACCGAA	Site-directed mutagenesis
F_ptamut	ATATAAGCTTCGAGATGCGTGATCGGCAC	Δ*pta* construction
R_ptamut	ATATGAATTCCACCACGGCGTATTTCAGC	Δ*pta* construction
F_ackAmut	ATATAAGCTTTCCCCGACCTCAACACCG	Δ*ackA* construction
R_ackArec	CGCAGTCGGTGGATGTAGACGAACGTCTTGCCGCCGTG	Δ*ackA* construction
F_ackArec	CACGGCGGCAAGACGTTCGTCTACATCCACCGACTGCG	Δ*ackA* construction
R_ackAmut	ATATCGCCGAAATCCTCCGCAG	Δ*ackA* construction
F_acsA1mut	ATATAAGCTTCGCAGGTTGACCTTGTGCC	Δ*acsA1* construction
R_acsA1rec	GTTTGGCGATGGGCGAGAGTCTGCCAGGACAACCGC	Δ*acsA1* construction
F_acsA1rec	GCGGTTGTCCTGGCAGACTCTCGCCCATCGCCAAAC	Δ*acsA1* construction
R_acsA1mut	ATATTGGTCGGCATGATCCACGG	Δ*acsA1* construction
F_glnRmut	ATATAAGCTTGCGTAGATGGCTGCTCCG	Δ*glnR* construction
R_glnRrec	GTCTGGTACGTCCTCGCCCACTACCCGTCTCCAACAGG	Δ*glnR* construction
F_glnR1rec	CCTGTTGGAGACGGGTAGTGGGCGAGGACGTACCAGAC	Δ*glnR* construction
R_glnRmut	ATATAGCTCACGCACCACCACC	Δ*glnR* construction
F_acsA1comp	ATATTCTAGAGACAGTTGCACCGCACCG	Δ*acsA1* complementation
R_acsA1comp	ATATAAGCTTCGGCACCATCGTCAACCAGG	Δ*acsA1* complementation
F_TAMRA_pUC19	GTTTTCCCAGTCACGACGTTGTA	DNase I footprinting
F_acsA1FootR	ATATGAATTCCGCAGGTTGACCTTGTGCC	DNase I footprinting
R_ acsA1FootR	ATATAAGCTTCGGCGGATAGGCTGACGG	DNase I footprinting
F_crp2over	ATATCATATGGACGAAGTGCTGGCGC	*crp2* overexpression
R_crp2over	ATATAAGCTTTCAGTGATGGTGATGGTGATGGTTCGCGCGCCGCGCGAG	*crp2* overexpression
F_sigA_RT	CTTGAGGTGACCGACGATCT	qRT-PCR
R_sigA_RT	AGCTTCTTCTTCCTCGTCCT	qRT-PCR
F_acsA1_RT	CCAAGCGGTTGTCCTGGCAG	qRT-PCR
R_ acsA1_RT	GGTTCGCCTTCCCAGTGGATG	qRT-PCR

Materials and Methods

Bacterial strains, plasmids, and culture conditions

The bacterial strains and plasmids used in this study are listed in Table 1. *E. coli* strains were grown in Luria-Bertani (LB) medium at 37°C. *M. smegmatis* strains were grown in Middlebrook 7H9 medium (Difco) supplemented with 10 mM glucose (7H9-glucose), 10 mM acetate (7H9-acetate), or 10 mM propionate (7H9-propionate) as a carbon source and 0.02% (v/v) Tween 80 as an anti-clumping agent at 37°C. *M. smegmatis* strains were grown aerobically in a 250-ml flask filled with 50 ml of growth medium on a gyratory shaker (200 rpm). Ampicillin (100 μg/ml for *E. coli*), kanamycin (50 μg/ml for *E. coli* and 15 μg/ml or 30 μg/ml for *M. smegmatis*), and hygromycin (200 μg/ml for *E. coli* and 50 or 25 μg/ml for *M. smegmatis*) were added to the growth medium when required.

DNA manipulation and electroporation

Standard protocols and manufacturers' instructions were followed for recombinant DNA manipulations (Green and Sambrook, 2012). Transformation of *M. smegmatis* with plasmids was carried out by electroporation as described elsewhere (Snapper *et al.*, 1990). The primers used for PCR and site-directed mutagenesis are listed in Table 2.

Construction of plasmids

(i) The temperature-sensitive suicide plasmids for the construction of mutant strains of *M. smegmatis*: to construct pKOTsΔpta, PCR was conducted with the F_ptamut and R_ptamut primers as well as the chromosomal DNA of *M. smegmatis* as a template. The amplified 2315-bp DNA fragment was restricted with HindIII and EcoRI and cloned into pUC19 digested with the same enzymes, yielding pUC19pta. The 1,365-bp DNA fragment within *pta* was excised from pUC19pta by restriction with BamHI, and the linear plasmid was self-ligated, resulting in pUC19Δpta. A 950-bp DNA fragment was amplified by PCR with the F_ptamut and R_ptamut primers and pUC19Δpta as a template. The product was digested with HindIII and cloned into pKOTs restricted with EcoRV and HindIII, resulting in pKOTsΔpta.

To construct pKOTsΔackA, two rounds of recombination PCR were performed. Using the chromosomal DNA of *M. smegmatis* as a template, two primary PCR reactions were performed with the primers F_ackAmut and R_ackArec, as well as with the primers F_ackArec and R_ackAmut to generate two 38-bp overlapping DNA fragments (448 and 504 bp, respectively). Both PCR products contain the same 609-bp deletion within *ackA* in the overlapping region. In the secondary PCR, a 914-bp DNA fragment with in-frame deletion of *ackA* was obtained using both the primary PCR products as templates and the F_ackAmut and R_ackAmut primers. The secondary PCR product was restricted with HindIII and cloned into pKOTs digested with EcoRV and HindIII, resulting in pKOTsΔackA.

To construct the pKOTsΔacsA1, two rounds of recombination PCR were conducted. Using the chromosomal DNA of *M. smegmatis* as a template, two primary PCR reactions were performed with the primers F_acsA1mut and R_acsA1rec, as well as with the primers F_acsA1rec and R_acsA1mut to generate two 36-bp overlapping DNA fragments (426 and 419 bp, respectively). Both PCR products contain the same 1,628-bp deletion within *acsA1* in the overlapping region. In the secondary PCR, an 809-bp DNA fragment with deletion of *acsA1* was obtained using both the primary PCR products as templates and the F_acsA1mut and R_acsA1mut primers. The secondary PCR product was restricted with HindIII and cloned into pKOTs digested with EcoRV and HindIII, yielding pKOTsΔacsA1.

To construct the pKOTsΔglnR, two rounds of recombination PCR were conducted. Using the chromosomal DNA of *M. smegmatis* as a template, two primary PCR reactions were performed with the primers F_glnRmut and R_glnRrec, as well as with the primers F_glnRrec and R_glnRmut to generate two 38-bp overlapping DNA fragments (426 and 497 bp, respectively). Both PCR products contain the same 572-bp deletion within *glnR* in the overlapping region. In the secondary PCR, an 885-bp DNA fragment with deletion of *glnR* was obtained using both the primary PCR products as templates and the F_glnRmut and R_glnRmut primers. The secondary PCR product was restricted with HindIII and cloned into pKOTs digested with EcoRV and HindIII, yielding pKOTsΔglnR.

(ii) pEMIIacsA1: to construct pEMIIacsA1, a DNA fragment comprising the 5' portion (99 bp) of *acsA1* and the 329-bp DNA sequence upstream of *acsA1* was amplified with the F_acsA1lacZ and R_acsA1lacZ primers using the chromosomal DNA of *M. smegmatis* as a template. The PCR product was restricted with ClaI and XbaI and cloned into pEMII, yielding pEMIIacsA1.

(iii) pBSIIacsA1: to construct pBSIIacsA1, PCR was conducted with the primers F_acsA1lacZ and R_acsA1lacZ as well as the pEMIIacsA1 as a template. The amplified 448-bp DNA fragment was restricted with ClaI and XbaI and cloned into pBluescript II KS+ digested with the same enzymes, yielding pBSIIacsA1.

(iv) pEMIIacsA1M: to construct the pEMIIacsA1-derived pEMIIasA1M plasmid with mutations in the CRP-binding site (CBS), PCR-based site-directed mutagenesis was performed with pBSIIacsA1 following the Quick Change site-directed mutagenesis procedure (Stratagene). Synthetic complementary oligonucleotides 33 bases long containing the substituted nucleotides in the middle of their sequences (F_acsA1_M and R_acsA1_M) were used to mutagenize the CRP-binding site, resulting in pBSIIacsA1M. The 437-bp ClaI-XbaI fragment from pBSIIacsA1M was cloned into pEMII, yielding pEMIIacsA1M. Mutations were verified by DNA sequencing.

(v) pT7-7Crp2: a 710-bp DNA fragment encompassing the *crp2* gene and six His codons immediately before its stop codon was amplified by PCR with the primers F_crp2over and R_crp2over using the chromosomal DNA of *M. smegmatis* as a template. The PCR product was restricted with NdeI and HindIII and cloned into pT7-7, yielding pT7-7crp2.

(vi) pUC19acsA1FootR: the plasmid was used as a template to generate TAMRA (6-carboxytetramethylrhodamine)-labeled DNA fragments containing the *acsA1* upstream region. For the construction of pUC19acsA1FootR, a 308-bp DNA fragment containing the CBS was amplified by PCR with the

F_acsA1FootR and R_acsA1FootR primers using the chromosomal DNA of *M. smegmatis* as a template. The PCR product was restricted with EcoRI and HindIII and cloned into pUC19, yielding pUC19acsA1FootR.

(vii) pMV306acsA1: pMV306acsA1 was used for complementation of the Δ*acsA1* mutant strain. To construct pMV306acsA1, a 2,598-bp DNA fragment containing the *acsA1* gene of *M. smegmatis* was amplified by PCR with the F_acsA1comp and R_acsA1comp primers using the chromosomal DNA of *M. smegmatis* as a template. The PCR product was restricted with XbaI and HindIII and cloned into pMV306, resulting in pMV306acsA1.

Construction of mutant strains of *M. smegmatis*

The Δ*pta*, Δ*ackA*, Δ*acsA1* and Δ*glnR* deletion mutants of *M. smegmatis* were constructed by allelic exchange mutagenesis using the corresponding pKOTs-derived suicide plasmids pKOTsΔpta, pKOTsΔackA, pKOTsΔacsA1, and pKOTsΔglnR, respectively, as described previously (Jeong *et al.*, 2013). In brief, the temperature-sensitive suicide plasmid was introduced into *M. smegmatis* by electroporation. Transformants were selected at 30°C (replication-permissive temperature) on 7H9-glucose agar plates containing hygromycin, and the selected transformants were grown in 7H9-glucose liquid medium supplemented with hygromycin for 3 days at 30°C. Heterogenotes of *M. smegmatis*, which were generated by a single recombination event, were selected for their hygromycin resistance on 7H9-glucose agar plates at 42°C (replication-nonpermissive temperature). The selected heterogenotes were grown on 7H9-glucose medium without antibiotics for 3 days at 37°C. Isogenic homogenotes were obtained from the heterogenotes after a second recombination by selecting them for sucrose resistance on 7H9-glucose agar plates containing 10% (w/v) sucrose at 37°C. The allelic exchange was verified by PCR with isolated genomic DNA.

RNA sequencing analysis

Comparative RNA sequencing analysis on the wild-type (WT) and Δ*crp1* mutant strains of *M. smegmatis* grown aerobically to an OD_{600} of 2.0–2.1 (late exponential phase) has been reported previously (Ko and Oh, 2020). For RNA sequencing analysis on the Δ*crp2* mutant, three biological replicate cultures of the WT and Δ*crp2* strains were grown aerobically to an OD_{600} of 2.0–2.1. Total RNA of each culture was isolated as described previously (Kim *et al.*, 2010). rRNA was removed from the isolated total RNA using a Ribo-Zero rRNA Removal Kit (Bacteria) (Illumina). The RNA sequencing libraries were created using a TruSeq RNA Sample Prep Kit v2 (Illumina) with the standard low-throughput protocol. Sequencing of the six libraries was conducted on an Illumina HiSeq 4000 platform at Macrogen Inc. using the Hiseq 3,000–4,000 sequencing protocol and TruSeq 3,000–4,000 SBS Kit v3 reagent (Illumina). Paired-end reads (101 bp) were then mapped to the reference genome sequence of *M. smegmatis* mc^2155 (GCF_000015005.1_ASM1500v1) with the program Bowtie 1.1.2 using default settings. The differentially expressed genes (DEGs) were subsequently identified pair-wise by the edgeR package in R language (Robinson *et al.*, 2010). The RNA sequencing data for the Δ*crp1* and Δ*crp2* mutants have been deposited in NCBI's Gene Expression Omnibus and are accessible through the GEO Series accession numbers GSE158137 and GSE203178, respectively.

β-Galactosidase assay and determination of the protein concentration

The β-Galactosidase activity was measured spectrophotometrically as described previously (Oh and Kaplan, 1999). The protein concentration was determined using a Bio-Rad protein assay kit (Bio-Rad) with bovine serum albumin (BSA) as a standard protein.

Quantitative real-time PCR

RNA isolation from *M. smegmatis* strains and cDNA synthesis were performed as described elsewhere (Kim *et al.*, 2010) except for the use of a random hexamer primer (ThermoFisher) in place of the gene-specific primers in cDNA synthesis. The contamination of DNA in the isolated RNA was checked by PCR with the primers to be used in quantitative real-time PCR (qRT-PCR). To determine the transcript levels of *acsA1* and *sigA*, qRT-PCR was performed in a 20-μl mixture containing 5 μl of the template cDNA, 15 pmol of each of two gene-specific primers, 10 μl of TB GreenTM Premix Ex TaqTM (Tli RNase Plus) (TaKaRa), 0.4 μl of the ROX passive fluorescent dye, and 2.6 μl of distilled water. Thermal cycling was initiated with 1 cycle at 95°C for 2 min, followed by 40 cycles of 95°C for 5 sec and 64°C for 30 sec. The *sigA* gene encoding the principal sigma factor was used as a reference gene for qRT-PCR to normalize the expression levels of *acsA1*. Melting curve analysis was performed for each reaction to examine whether a single PCR product was amplified during qRT-PCR. The primers used for qRT-PCR are listed in Table 2.

Protein purification

C-Terminally His_6-tagged Crp1 and Crp2 proteins were expressed in the *E. coli* BL21 (DE3) strain harboring the pT7-7 derivative plasmids pT7-7crp and pT7-7crp2, respectively. The strains harboring the pT7-7 derivatives were cultivated aerobically to an OD_{600} of 0.4–0.6 at 37°C in LB medium containing 100 μg/ml ampicillin. Expression of the *crp1* and *crp2* genes was induced by the addition of isopropyl-β-*D*-thiogalactopyranoside (IPTG) to the cultures to a final concentration of 0.5 Mm, and then cells were further grown for 4 h at 30°C. Cells were harvested from 300 ml cultures and resuspended in 10 ml of buffer A (20 Mm Tris-HCl; pH 8.0 and 200 mM NaCl) containing DNase I (10 U/ml) and 10 mM $MgCl_2$. The resuspended cells were disrupted twice using a French pressure cell, and cell-free crude extracts were obtained by centrifugation twice at 20,000 × *g* for 15 min. The crude extracts were loaded into a column packed with 500 μl of the 80% (v/v) slurry of Ni-Sepharose high-performance resin (GE Healthcare). The resin was washed with 40 bed volumes of buffer A containing 5 mM imidazole and washed further with 20 bed volumes of buffer A containing 60 mM imidazole. His_6-tagged CRP proteins were eluted from the resin with buffer A containing 250 mM imidazole. The eluted protein was desalted using a PD-10 desalting column (GE Healthcare) equilibrated with appropriate buffer.

DNase I footprinting analysis

DNase I footprinting was carried out using fluorescence (TAMRA)-labeled DNA fragments and purified Crp1 and Crp2 protein. A 341-bp TAMRA-labeled DNA fragment containing the *acsA1* upstream region was generated by PCR using the F_acsA1FootR and TAMRA-labeled F_TAMRA_pUC19 primers. The pUC19acsA1FootR plasmid was used for PCR as a template to generate the DNA fragments with the TAMRA-labeled noncoding strand. The PCR products were purified after agarose gel electrophoresis, and the DNA concentration was determined using a Multiskan SkyHigh Microplate spectrophotometer (ThermoFisher). DNA binding reaction mixtures were composed of 5 pmol of labeled DNA probes, various amounts of purified Crp1 or Crp2, 20 mM Tris-HCl (pH 8.0), 0.2 mM $MgCl_2$, 2.1 mM KCl, 0.04 mM DTT, 11.1% (v/v) glycerol, and 200 μM cAMP in a final volume of 190 μl. The mixture was incubated for 10 min at 25°C prior to DNase I treatment. DNase I treatment, DNA purification, and electrophoresis on 6% (w/v) denaturing polyacrylamide gels were performed as described previously (Ko and Oh, 2020). Reference sequencing was performed by using a Thermo sequenase dye primer manual cycle sequencing kit (ThermoFisher) with the primer F_TAMRA_pUC19 and the template plasmid pUC19acsA1FootR.

Results

Expression levels of the genes involved in acetate activation in the WT and CRP mutant strains of M. smegmatis

Mycobacterium smegmatis has the genes that encode the homologs of PTA, ACK, and ACS that are implicated in acetate activation (Fig. 1A). The *pta* (*MSMEG_0783*) and *ackA* (*MSMEG_0784*) genes encode PTA and ACK, respectively. The *pta* gene is expected to form an operon with the downstream *ackA* gene in *M. smegmatis* as in other bacteria (Kakuda *et al.*, 1994; Reinscheid *et al.*, 1999; Rücker *et al.*, 2015). *Mycobacterium smegmatis* has four genes (*MSMEG_6179*, *acsA1*; *MSMEG_0718*, *acsA2*; *MSMEG_3986*, *acsA3*; *MSMEG_5650*, *acsA4*) encoding ACS. The relative expression levels of *acsA1*, *acsA2*, *acsA3*, and *acsA4* were extrapolated from their reads per kilo base pair per million mapped reads (RPKM) values obtained from our previous RNA sequencing analysis on the WT strain of *M. smegmatis* grown on glucose as the sole carbon source (Lee *et al.*, 2018). The RPKM values of *acsA1*, *acsA2*, *acsA3*, and *acsA4* indicated that the transcript level of *acsA1* in the WT strain was much higher than those of *acsA2*, *acsA3*, and *acsA4* (Fig. 1B). The result implies that AcsA1 is the predominantly expressed ACS in *M. smegmatis*. The genome of *M. smegmatis* has two genes (*MSMEG_6189*, *crp1*; *MSMEG_0539*, *crp2*) encoding CRP. Our RNA sequencing analysis using the WT, Δ*crp1*, and Δ*crp2* mutants of *M. smegmatis* revealed that expression of the *acsA1* and *acsA4* genes were derepressed in Δ*crp1* mutant by 6.1- and 16.8-fold relative to the WT strain, respectively, when the strains were aerobically grown on glucose as the sole carbon source (Fig. 1B). Deletion of *crp2* resulted in a much less derepression of *acsA1* and *acsA4* relative to their expression in the WT strain than that of *crp1*. These results suggest that CRP, especially Crp1, is likely to be involved in repression of *acsA1 and acsA4*. In contrast, expression of the *pta-ack* operon was rather slightly decreased in the Δ*crp1* and Δ*crp2* mutants compared to that in the WT strain. Besides acetate activation, the

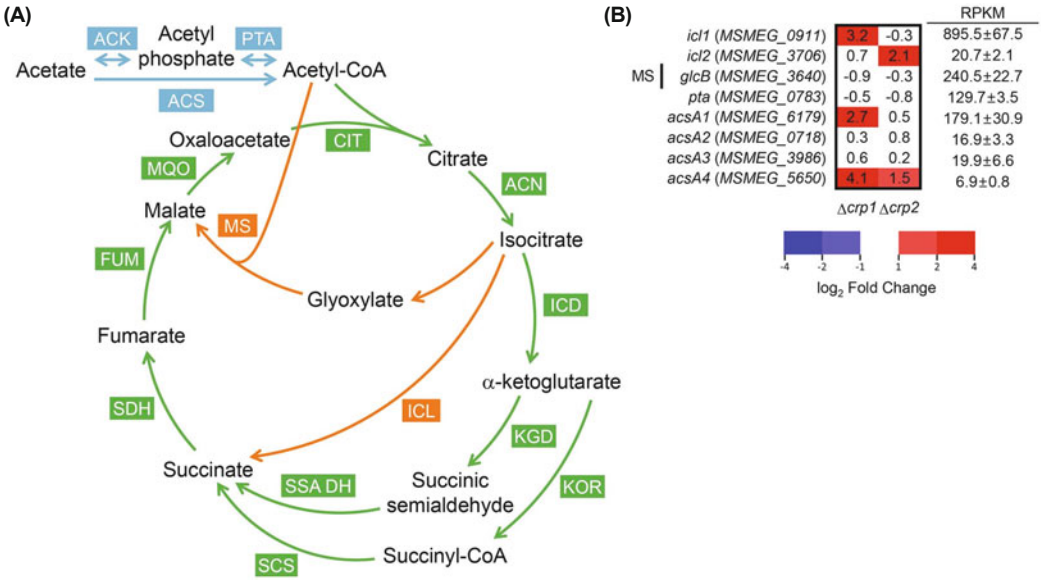

Fig. 1. The scheme of acetate metabolism in *M. smegmatis* and the heatmap showing the fold change (FC) in expression of the genes involved in acetate activation and the glyoxylate shunt in the Δ*crp1* and Δ*crp2* mutants relative to that of the WT strain. (A) The acetate activation pathways, glyoxylate shunt, and TCA cycle are marked in blue, orange, and green, respectively. (B) Relative expression levels of the genes involved in acetate activation and the glyoxylate shunt in the Δ*crp1* and Δ*crp2* mutants relative to that in the WT strain are visualized using the heatmap and the numbers indicating the $\log_2$ FC in gene expression. The RPKM values of the genes in the WT strain grown aerobically to an OD_{600} of 0.4–0.5 are indicated next to the heat map (Lee *et al.*, 2018). ACK, acetate kinase; PTA, phosphotransacetylase; ACS, acetyl-CoA synthase; ICL, isocitrate lyase; MS, malate synthase; CIT, citrate synthase; ACN, aconitase; ICD, isocitrate dehydrogenase; KGD, α-ketoglutarate decarboxylase; KOR, α-ketoglutarate,ferredoxin oxidoreductase; SSA DH; succinic semialdehyde dehydrogenase; SCS, succinyl-CoA synthetase; SDH, succinate dehydrogenase; FUM, fumarate dehydrogenase; MQO, malate,quinone oxidoreductase.

glyoxylate shunt consisting of two reactions catalyzed by isocitrate lyase (ICL) and malate synthase (MS) is required for *M. smegmatis* to grow on acetate as the sole carbon source (Fig. 1A) (Ko *et al.*, 2021). As shown in Fig. 1B, RNA sequencing analysis confirmed our previous report that the *icl1* gene encoding the major ICL is under the negative regulation of Crp1 (Ko *et al.*, 2021).

Since AcsA1 appears to be the predominantly expressed ACS and under the negative regulation of CRP in *M. smegmatis*, we focused on the regulation of *acsA1* expression by CRP in this study.

Roles of the ACK-PTA and ACS pathways in acetate utilization

There are two possible pathways for acetate activation from acetate to acetyl-CoA in *M. smegmatis*, the ACK-PTA and ACS pathways (Fig. 1A). To determine which pathway is more important for acetate activation, we first constructed null mutants of *M. smegmatis* carrying a deletion within *pta*, *ackA*, or *acsA1*. The WT and mutant strains were assessed for their growth in 7H9 medium supplemented with glucose or acetate as the sole carbon source to examine the roles of the *pta*, *ackA*, and *acsA1* genes in utilization of acetate in *M. smegmaits*. No difference between the WT, Δ*pta*, Δ*ackA*, and Δ*acsA1* mutant strains was observed regarding the growth rate when the strains were grown on glucose (Fig. 2A). When acetate was supplied as the sole carbon source, the growth rate of the Δ*pta* and Δ*ackA* mutants was comparable to that of WT (Fig. 2B). In contrast, the Δ*acsA1* mutant strain showed significantly retarded growth compared to the WT strain when acetate was supplied as the sole carbon source (Fig. 2B). Since the mycobacterial ACSs also possess the activity of propionyl-CoA synthetase (Li *et al.*, 2011; Liu *et al.*, 2018), we examined whether deletion of *acsA1* affects growth of *M. smegmatis* on propionate. As shown in Fig. 2C, the Δ*acsA1* strain showed the growth rate comparable to that of the WT strain in 7H9-propionate, which is likely to be due to the presence of propionyl-CoA synthetase (PrpE: MSMEG_5404) in *M. smegmatis*. Inactivation of the *pta* or *ackA* gene did not affect the growth of *M. smegmatis* on propionate, either (Fig. 2C). Introduction of the pMV306acsA1 plasmid carrying the intact *acsA1* gene into the Δ*acsA1* mutant restored growth of the mutant on acetate to the WT level (Fig. 2D), indicating that the defect in acetate utilization observed for the Δ*acsA1* mutant was the result of *acsA1* inactivation. Taken together, these results indicate that the ACS pathway serves as the major pathway for acetate activation and that AcsA1 is important for acetate activation in *M. smegmatis* during growth on acetate.

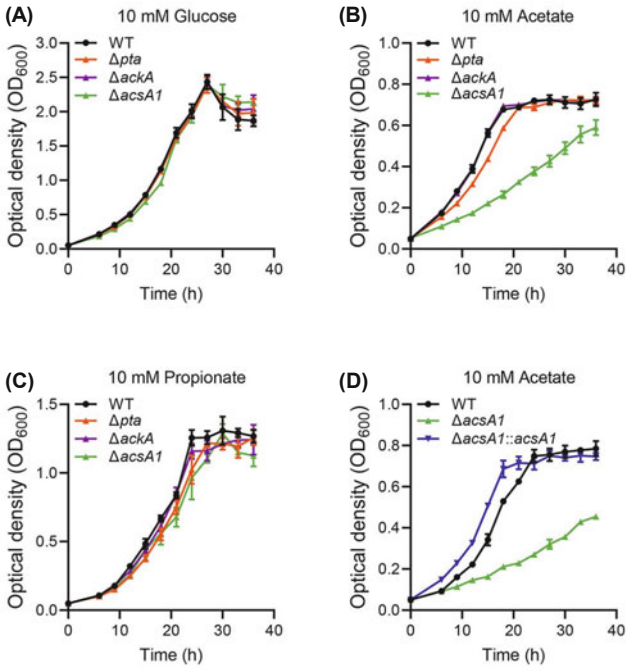

Fig. 2. Growth of the WT, Δ*pta*, Δ*ackA*, and Δ*acsA1* strains of *M. smegmatis* on glucose, acetate or propionate as the sole carbon source. The WT and mutant strains of *M. smegmatis* were grown aerobically at 37°C in 7H9 medium supplemented with 10 mM glucose (A), 10 mM acetate (B), or 10 mM propionate (C) as the sole carbon source. (D) For complementation of the Δ*acsA1* mutant, pMV306acsA1 (a pMV306-derived plasmid carrying the intact *acsA1* gene and its own promoter) was introduced into the mutant. The Δ*acsA1* mutant harboring pMV306acsA1 (Δ*acsA1*::*acsA1*), as well as the WT and Δ*acsA1* strains with the empty vector pMV306, was grown aerobically in 7H9-acetate. Growth of the strains was measured spectrophotometrically at 600 nm at the indicated time points. All values provided were determined from three biological replicates. The error bars indicate the standard deviations.

Negative regulation of the *acsA1* gene by Crp1

RNA sequencing analysis showed that expression of *acsA1* was significantly (6.1-fold) and marginally (1.5-fold) higher

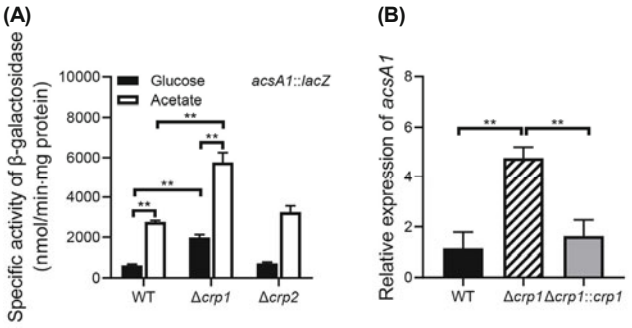

Fig. 3. Expression levels of the *acsA1* gene in the WT, Δ*crp1*, and Δ*crp2* strains of *M. smegmatis*. (A) The WT, Δ*crp1*, and Δ*crp2* strains containing the *acsA1*::*lacZ* translational fusion plasmid pEMIIacsA1 were grown aerobically to an OD_{600} of 0.45 to 0.5 in 7H9 medium supplemented with 10 mM glucose or 10 mM acetate as the sole carbon source. Cell-free crude extracts were used to measure β-galactosidase activity. (B) Complementation of the Δ*crp1* mutant. For complementation of the Δ*crp1* mutant, pMV306crp (a pMV306-derived plasmid carrying the intact *crp1* gene and its own promoter) was introduced into the mutant. As control strains, the WT and Δ*crp1* strains with the empty vector pMV306 were used in the experiment. All the strains were grown aerobically to an OD_{600} of 0.45–0.5 in 7H9 medium supplemented with 10 mM glucose as the sole carbon source. The expression level of *acsA1* was quantitatively determined by qRT-PCR and normalized to *sigA* (the gene encoding the principal sigma factor) expression. The expression level of *acsA1* in the WT strain grown in 7H9-glucose medium was set at 1, and the relative values were expressed for the mutant strains. All values provided were determined from three biological replicates. The error bars indicate the standard deviations. ** $p < 0.01$.

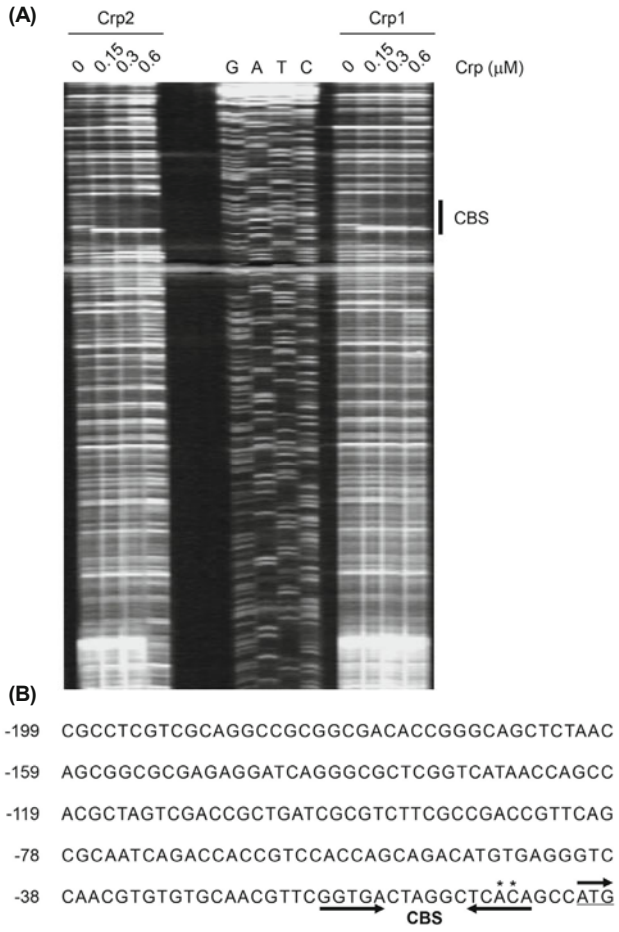

Fig. 4. Binding of Crp1 and Crp2 to the *acsA1* regulatory region. (A) DNase I footprinting analysis of the *acsA1* regulatory region bound by purified Crp1 and Crp2. The DNA fragments containing the noncoding strand labeled with TAMRA at their 5' ends were incubated with increasing concentrations of purified Crp1 or Crp2 (0.15, 0.3, and 0.6 μM) in the presence of 200 μM cAMP and then subjected to DNase I footprinting reactions. The regions protected by Crp1 or Crp2, which indicate the CRP-binding sites (CBS), are marked by a thick black line. Lanes G, A, T, and C represent the sequence ladders. (B) The upstream sequence of the *acsA1* gene showing its start codon and identified CRP-binding site. The start codon of *acsA1* is indicated by the underline and the arrow indicating the transcriptional direction. The numbers on the left side of the sequence show the positions of the leftmost nucleotides relative to the first nucleotide of the *acsA1* gene. The nucleotides within the CBS, which underwent site-directed mutagenesis, are indicated by *.

in the Δ*crp1* and Δ*crp2* mutants than that in the WT strain, respectively. Using an *acsA1-lacZ* translational fusion, we examined whether *acsA1* expression is induced in *M. smegmatis* grown on acetate and whether Crp1 and Crp2 are involved in the regulation of *acsA1* expression. As shown in Fig. 3A, expression of *acsA1* was induced by 4.4-fold in WT grown on acetate relative to that in WT grown on glucose. Expression of *acsA1* was shown to be derepressed in the Δ*crp1* mutant compared to that in the WT strain under both glucose and acetate conditions. On the other hand, the Δ*crp2* mutant showed *acsA1* expression comparable to the WT strain under both glucose and acetate conditions. The fold change in derepression of *acsA1* in the Δ*crp1* mutant relative to the WT strain was shown to be smaller under acetate conditions than that under glucose conditions. These results indicate that the major Crp1 negatively regulates the expression of *acsA1* in *M. smegmatis* during growth on glucose and acetate and that its repression effect is greater under glucose conditions. It is noteworthy that expression of *acsA1* was still 2.9-fold induced in the Δ*crp1* mutant under acetate condition compared to the same mutant strain grown under glucose condition. Our qRT-PCR analysis showed that introduction of the intact *crp1* gene into the Δ*crp1* mutant led to restoration of *acsA1* expression to that observed in the WT strain when the strains were grown on glucose (Fig. 3B), indicating that derepression of *acsA1* observed in the Δ*crp1* mutant resulted from null mutation of *crp1*.

To identify the CRP-binding site(s) in the upstream region of *acsA1*, DNase I footprinting analysis was conducted with purified Crp1 or Crp2 and TAMRA-labeled DNA fragments containing the *acsA1* upstream region. In the presence of 200 μM cAMP in the reaction mixtures, the presence of Crp1 or Crp2 in the reaction mixtures protected an 18-bp DNA region from DNase I cleavage at position proximal to the start codon of *acsA1* (Fig. 4A and B). The protected region contains a putative CRP-binding sequence (CBS: GGTGA-N_6-TCACA) that is similar to the known CRP-binding consensus sequence (TGTGA-N_6-TCACA) (Fig. 4B). To examine the role of the identified CBS in the regulation of *acsA1* expression in *M. smegmatis*, we determined the effect of CBS mutation on *acsA1* expression in the WT strain of *M. smegmatis* grown on glucose or acetate by using pEMIIacsA1M that contains mutations within CBS (Fig. 5). Two transition mutations were introduced into the CBS (GGTGA-N_6-TCACA to GGTGA-N_6-TCGTA) on pEMIIacsA1 to construct pEMIIacsA1M (the mutated nucleotides are marked by underlines). Since the CBS is located close to the start codon of *acsA1* gene (Fig. 4B), the right half site of CBS was mutated to avoid mutation of the ribosome binding site. As expected, expression of *acsA1* was

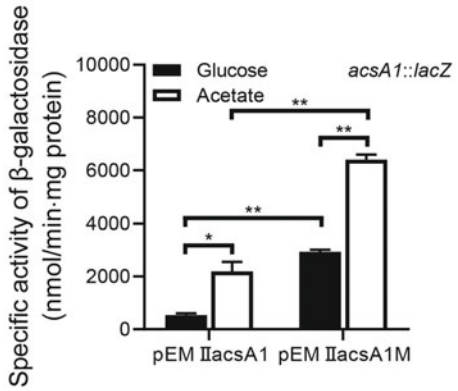

Fig. 5. Effects of mutation in the identified CBS on *acsA1* expression. The *acsA1* promoter activity was determined by using the pEMIIacsA1-derived translational fusion plasmid pEMIIacsA1M with mutation within the CBS, as well as pEMIIacsA1 as a control. The WT strains of *M. smegmatis* harboring the translational fusion plasmids were grown aerobically to an OD_{600} of 0.45 to 0.5 in 7H9 medium supplemented with 10 mM glucose or 10 mM acetate as the sole carbon source. Cell-free crude extracts were used to measure β-galactosidase activity. All values provided were determined from three biological replicates. The error bars indicate the standard deviations. *$p < 0.05$; **$p < 0.01$.

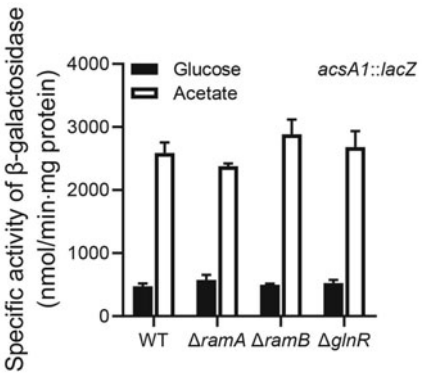

Fig. 6. Expression levels of the *acsA1* gene in the WT, Δ*ramA*, Δ*ramB*, and Δ*glnR* strains. The WT and mutant strains containing pEMIIacsA1 were grown aerobically to an OD_{600} of 0.45 to 0.5 in 7H9 medium supplemented with 10 mM glucose or 10 mM acetate as the sole carbon source. Cell-free crude extracts were used to measure β-galactosidase activity. All values provided were determined from three biological replicates. The error bars indicate the standard deviations.

strongly induced by acetate in the control WT strain with pEMIIacsA1. Under both glucose and acetate conditions, expression of *acsA1* from pEMIIacsA1M was significantly increased compared to that from pEMIIacsA1 (Fig. 5). Derepression of *acsA1* by CBS mutation occurred to a degree similar to that observed for the Δ*crp1* mutant relative to the WT strain (see Figs. 3A and 5). These results clearly indicate that the identified CBS serves as the binding site of CRP for repression of *acsA1* expression.

As shown in Figs. 3A and 5, expression of *acsA1* was still induced by acetate in the Δ*crp1* mutant and the WT strain carrying the CBS-mutated pEMIIacsA1M, suggesting that (an) additional regulatory system(s) other than CRP might operate to induce *acsA1* expression in *M. smegmatis* during growth on acetate. It has been demonstrated in *Corynebacterium glutamicum* that the LuxR-type transcriptional regulator RamA (Cg2831: regulator of acetate metabolism A) serves as an activator in the acetate-inducible genes involved in acetate metabolism such as *aceA* encoding ICL, *pta*, and *ack* (Cramer *et al.*, 2006; Auchter *et al.*, 2011). *M. smegmatis* possesses the RamA homolog (MSMEG_5651) that shares 38% sequence identity and 57% similarity with RamA of *C. glutamicum*. In *M. smegmatis*, *M. tuberculosis*, and *C. glutamicum*, the *aceA* and *icl1* genes have been demonstrated to be upregulated during growth on acetate, which is achieved by RamB-mediated induction of the genes in the presence of acetate (Gerstmeir *et al.*, 2004; Micklinghoff *et al.*, 2009; Auchter *et al.*, 2011; Ko *et al.*, 2021). There is another known transcriptional regulator GlnR that has been reported to negatively regulate the acetate-inducible *icl1* gene and the *prpDBC* operon involved in the methylcitrate cycle in *M. smegmatis* under nitrogen-limiting conditions (Liu *et al.*, 2019; Qi *et al.*, 2021). GlnR has been also shown to serve as an activator for expression of *acsA1*, *prpE* encoding propionyl-CoA synthetase, and *pat* encoding protein acetyltransferase under nitrogen-limiting conditions (Liu *et al.*, 2018). To ascertain the involvement of RamA, RamB, and GlnR in the regulation of *acsA1* expression, the expression level of *acsA1* was determined in the WT, Δ*ramA*, Δ*ramB*, and Δ*glnR* strains of *M. smegmatis* carrying pEMIIacsA1. When expression of *acsA1* in the WT strain was compared to that in the Δ*ramA*, Δ*ramB*, and Δ*glnR* mutants of *M. smegmatis*, inactivation of *ramA*, *ramB* and *glnR* did not result in noticeable changes in *acsA1* expression in *M. smegmatis* under both glucose and acetate conditions (Fig. 6). These results indicate that none of RamA, RamB, and GlnR is involved in the regulation and induction of *acsA1* expression under acetate conditions in *M. smegmatis*.

A decrease in *acsA1* expression under respiration-inhibitory conditions

The Δaa_3 mutant strain of *M. smegmatis* lacking the aa_3 cytochrome *c* oxidase of the respiratory ETC has been reported to exhibit a reduced respiration rate by ~50% (Jeong *et al.*, 2018). The intracellular level of cAMP has been demonstrated to increase in the Δaa_3 mutant strain of *M. smegmatis* compared to that in the WT strain, which was shown to accompany with an increase in expression of genes under the positive regulation of Crp1 in the mutant (Ko and Oh, 2020). Since expression of *acsA1* is negatively regulated by Crp1 like that of *icl1* (Ko *et al.*, 2021), we assumed that expression of *acsA1* and *icl1* would be reduced in the Δaa_3 mutant strain relative to that in the WT strain. As ACS is important for utilization of acetate, so ICL of the glyoxylate shunt is also crucial for *M. smegmatis* to grow on acetate, which is because the glyoxylate shunt is only the anaplerotic pathway that replenishes intermediates of the TCA cycle from acetyl-CoA in *M. smegmatis* grown on acetate as the sole carbon source. If our assumption is correct, the ability of the Δaa_3 mutant to grow on acetate would be compromised compared to that of the WT strain. To examine this assumption, growth of the WT and Δaa_3 mutant strains was compared in 7H9 medium supplemented with glucose or acetate as the sole carbon source. When glucose was supplemented as the sole carbon source, the Δaa_3 mutant carrying the empty vector pMV306 showed the slower growth and reached the stationary phase at a lower cell density than the WT strain with pMV306 probably due to the reduced respiration rate as reported previously (Jeong *et al.*, 2018) (Fig. 7A). When acetate was the sole carbon source, growth of the Δaa_3 strain with pMV306 was severely impaired compared to the WT strain with pMV306 (Fig. 7B). Consistent with this result, the Δaa_3 mutant did not form colonies on the solid 7H9-acetate plate (data not shown). Introduction of the pMV306ctaC plasmid carrying the intact *ctaC* gene into the Δaa_3 mutant restored growth of the mutant on both glucose and acetate to the WT level (Fig. 7A and B), indicating that the severe defect in acetate utilization observed for the Δaa_3 mutant is due to inactivation of the *ctaC* gene encoding subunit II of the aa_3 cytochrome *c* oxidase. Next, expression of *acsA1* and *icl1* genes was examined in the WT and Δaa_3 mutant strains of *M. smegmatis* carrying pEMIIacsA1 and pEMIIicl1, respectively (Fig. 7C). Because the Δaa_3 mutant strain barely grew under acetate conditions, the WT and Δaa_3 mutant strains were cultivated under acetate conditions as follows: the WT and Δaa_3 mutant strains with pEMIIacsA1 or pEMIIicl1 were first grown to an OD_{600} of 0.3 in 7H9-glucose medium, harvested and washed twice with 7H9 medium without carbon source, followed by further cultivation for 3 h in 7H9-acetate medium. Under acetate conditions, expression of *acsA1* and *icl1* was reduced in the Δaa_3 mutant

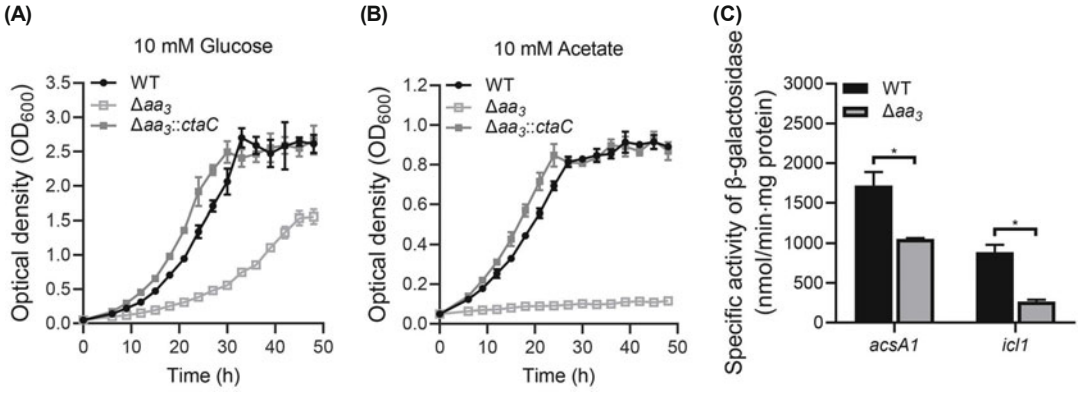

Fig. 7. Growth of the WT and Δ*aa*$_3$ strains of *M. smegmatis* on glucose or acetate as the sole carbon source and expression levels of *acsA1* and *icl1* in the WT and Δ*aa*$_3$ strains. The WT and Δ*aa*$_3$ strains containing pMV306, as well as the complemented Δ*aa*$_3$ strain with pMV306ctaC (Δ*aa*$_3$::*ctaC*), were grown aerobically in 7H9 medium supplemented with 10 mM glucose (A) or 10 mM acetate (B). Growth of the strains was measured spectrophotometrically at 600 nm at the indicated time points. (C) Expression levels of *acsA1* and *icl1* in the WT and Δ*aa*$_3$ strains. To determine the expression levels of *acsA1* and *icl1* in the strains grown on acetate, the WT and Δ*aa*$_3$ strains with pEMIIacsA1 and pEMIIicl1, respectively, were grown aerobically to an OD_{600} of 0.3 in 7H9-glucose medium. The cultures were harvested and washed twice with 7H9 medium to remove glucose. The washed cells were resuspended in 7H9-acetate medium and further grown aerobically for 3 h. Cell-free crude extracts were used to measure β-galactosidase activity. All values provided were determined from three biological replicates. The error bars indicate the standard deviations. *$p < 0.05$.

by 39% and 70%, respectively, compared to that in the WT strain. Taken together, the results imply that acetate activation and the glyoxylate shunt operate less efficiently in *M. smegmatis* under respiration-inhibitory conditions, which results in detrimental effects on growth of *M. smegmatis* on acetate as the sole carbon source.

Discussion

In this study, we demonstrated that AcsA1 (MSMEG_6179) functions as the major ACS in acetate activation required for growth of *M. smegmatis* on acetate as the sole carbon source. This suggestion was extrapolated from the much higher RPKM value of AcsA1 than those of the other ACSs (MSMEG_0718, MSMEG_3986, and MSMEG_5650) (Fig. 1B) and the compromised growth of Δ*acsA1* mutant of *M. smegmatis* on acetate as the sole carbon source (Fig. 2B). Among the four ACS genes found in *M. smegmatis*, our RNA sequencing result showed that *acsA1* and *acsA4* (*MSMEG_5650*) are under the negative regulation of CRP (Fig. 1B). Recently, Liu *et al.* (2018) reported that expression of *acsA1* and *acsA4* are acetate-inducible, while expression of *acsA2* (*MSMEG_0718*) and *acsA3* (*MSMEG_3986*) is relatively constitutive. Importantly, we have recently suggested that Crp1 is implicated in induction of the acetate-inducible *icl1* gene encoding the major ICL in acetate-grown *M. smegmatis* (Ko *et al.*, 2021). These findings allowed us to assume that acetate inducibility of *acsA1* and *acsA4* might be related to CRP. Since the expression extent of *acsA4* was found to be very low compared to that of *acsA1* (the RPKM values of *acsA1* and *acsA4* are 179. 1 and 6.9. respectively), we focused on studying expression of *acsA1* in this study. Our RNA sequencing analysis and reporter gene assay showed that expression of *acsA1* is derepressed in the Δ*crp1* mutant relative to that in the WT strain when the strains were grown on glucose (Figs. 1B and 3A). Derepression of *acsA1* was also observed to occur in the Δ*crp1* mutant during growth on acetate (Fig. 3A). DNase I footprinting analysis and site-directed mutagenesis revealed that the upstream region of *acsA1* possesses a CBS which contains the sequence (GGTGA-N_6-TCACA) that is similar to the known CRP-binding motif (TGTGA-N_6-TCACA) and centered at position -11.5 relative to the start codon of *acsA1* (Figs. 4 and 5). The position of the identified CBS implies that the binding of CRP to its binding site hinders the initial elongation step or the formation of the open complex during transcription, leading to repression of *acsA1* expression. Although both Crp1 and Crp2 have the ability to bind to the identified CBS as shown in Fig. 4, our result showed that only Crp1 serves as a repressor of *acsA1* expression (Fig. 3A), which is probably because Crp1 is the major CRP with much higher expression than Crp2 (Ko and Oh, 2020). Taken together, our findings clearly indicate that Crp1 serves as a repressor for expression of *acsA1*. The cellular levels of cAMP in the WT strain grown on glucose have been demonstrated to be approximately two-fold higher than those in the WT grown on acetate (Ko *et al.*, 2021). Increased cAMP levels in glucose-grown cells are assumed to enhance the functionality of Crp1, which in turn leads to more repression of *acsA1* in glucose-grown *M. smegmatis* than in acetate-grown *M. smegmatis*. This assumption explains a possible mechanism underlying CRP-mediated induction of *acsA1* expression under acetate conditions. Since we failed to obtain a Δ*crp1*Δ*crp2* double mutant of *M. smegmatis* probably due to the indispensability of CRP for growth of *M. smegmatis*, the implication of CRP in the regulation of *acsA1* expression had to be examined using the Δ*crp1* mutant. Due to the presence of Crp2 in the Δ*crp1* mutant, it is possible that the role of CRP in induction of *acsA1* expression under acetate-growth conditions might be underestimated and that the observed induction of *acsA1* expression in the Δ*crp1* mutant might be attributable to Crp2. However, the finding that induction of *acsA1* expression also occurred in the WT strain carrying pEMIIacsA1M with CBS mutation

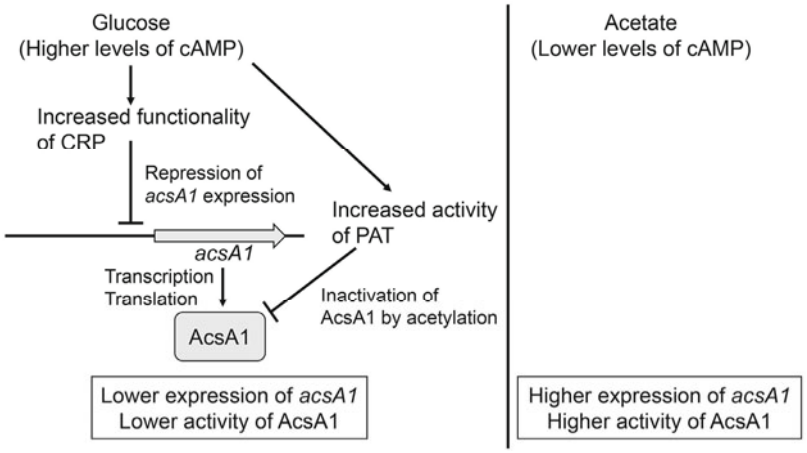

Fig. 8. Model for the transcriptional and post-transcriptional regulation of *acsA1* by changes in cAMP levels in *M. smegmatis* grown on glucose or acetate as the sole carbon source. CRP, cAMP receptor protein; PAT, lysine acetyltransferase.

during growth on acetate (Fig. 5) strongly indicates that in addition to CRP, there is another regulatory system that is involved in induction of *acsA1* expression by acetate. Our reporter gene assays using the Δ*ramA*, Δ*ramB*, and Δ*glnR* presented in Fig. 6 suggest that the RamA, RamB, and GlnR transcriptional regulators, which are known to be involved in the regulation of acetate-inducible genes, are not responsible for acetate-inducible expression of *acsA1* in *M. smegmatis*. Further study is required to identify a regulatory system other than CRP, which is implicated in upregulation of *acsA1* expression under acetate conditions relative to under glucose conditions.

Besides the regulation of *acsA1* expression by CRP, intracellular cAMP levels are likely to influence acetate metabolism through the cAMP-dependent allosteric activation of PAT that inactivates AcsA1 and Icl1 in *M. smegmatis* by acetylation (Hayden *et al.*, 2013; Liu *et al.*, 2018; Xu *et al.*, 2018). The PAT protein (MSMEG_5458 in *M. smegmatis*) belongs to GCN5-related *N*-acetyltransferase (GNAT) superfamily and catalyzes acetyl transfer from acetyl-CoA to its target proteins (Nambi *et al.*, 2010, 2012; Liu *et al.*, 2018). It consists of an N-terminal cAMP-binding domain and a C-terminal GNAT domain and requires the binding of cAMP to the N-terminal domain for its catalytic activity (Nambi *et al.*, 2010, 2012; Hayden *et al.*, 2013; Liu *et al.*, 2018). Based on our results in conjunction with the previous reports regarding PAT (Nambi *et al.*, 2010, 2012; Hayden *et al.*, 2013; Liu *et al.*, 2018), we present a model explaining the enhancement of acetate activation in *M. smegmatis* grown on acetate relative to *M. smegmatis* grown on glucose (Fig. 8). When *M. smegmatis* is grown on glucose as the sole carbon source, intracellular cAMP levels are increased by two-fold compared to those in *M. smegmatis* grown on acetate (Ko *et al.*, 2021). The activity of both CRP and PAT is expected to increase by allosteric activation resulting from the increased cAMP levels, thereby leading to the reduced expression of *acsA1* and the reduced activity of AcsA1 by acetylation in *M. smegmatis* grown on glucose. Conversely, reduced cAMP levels in *M. smegmatis* grown on acetate cause both an increase in *acsA1* expression and alleviation of the PAT-mediated inactivation of AcsA1, which ultimately results in enhanced acetate activation. In agreement with this model, the Δaa_3 mutant, in which cAMP levels have been reported to increase by 3.2-fold relative to the WT strain (Ko and Oh, 2020), showed the decreased expression of *acsA1* and *icl1* that are under the negative regulation of Crp1 (Ko *et al.*, 2021). The observed severely impaired growth of Δaa_3 mutant on acetate as the sole carbon source is likely to result from combined effects of reduced expression of *acsA1* and *icl1* by CRP, inhibition of acetate metabolism by the activation of PAT, and growth retardation by respiration inhibition in the mutant.

During host infection, *M. tuberculosis* has been suggested to utilize fatty acids and cholesterol as important carbon sources (Bloch and Segal, 1956; Pandey and Sassetti, 2008; Lee *et al.*, 2013; VanderVen *et al.*, 2015). Low oxygen tensions and pH in granulomas are expected to inhibit the respiratory ETC of *M. tuberculosis*, leading to less efficient operation of the TCA cycle. Under these conditions, the ACK-PTA pathway operates to generate acetate from acetyl-CoA to mitigate toxic effects of acetyl-CoA accumulation in the bacterial cell (Brown *et al.*, 1977; Sadykov *et al.*, 2013; Enjalbert *et al.*, 2017). Unless acetate activation by ACS is inhibited under respiration-inhibitory conditions, removal of acetyl-CoA would be hampered by the futile cycle of the interconversion between acetyl-CoA and acetate. If expression of *acs* is under the negative regulation of CRP in *M. tuberculosis* like that in *M. smegmatis*, CRP-mediated repression of *acs* under respirationnhibitory conditions might help *M. tuberculosis* avoid the futile cycle to enhance the growth fitness under the conditions. Further study is required to reveal whether the gene encoding ACS is regulated by CRP in *M. tuberculosis*.

In conclusion, we here demonstrated that AcsA1 is the major ACS among four ACSs found in *M. smegmatis*. Expression of *acsA1* was demonstrated to be induced during growth on acetate compared to that during growth on glucose. The *acsA1* gene was shown to be under the negative regulation of CRP, which contributes to some extent to the induction of *acsA1* expression under acetate conditions. We also demonstrated that inhibition of the ETC led to the severely compromised growth of *M. smegmatis* on acetate as the sole carbon source, which might result from both a decrease in *acsA1* and *icl1* expression through the activation of CRP and the inactivation of AcsA1 and Icl1 through their acetylation by PAT.

Acknowledgements

This work was supported by a 2-years Research Grant of Pusan National University to JIO.

Conflict of Interest

The authors declare that they have no conflicts of interest with the contents of this article.

References

Auchter, M., Cramer, A., Huser, A., Ruckert, C., Emer, D., Schwarz, P., Arndt, A., Lange, C., Kalinowski, J., Wendisch, V.F., and Eikmanns, B.J. 2011. RamA and RamB are global transcriptional regulators in *Corynebacterium glutamicum* and control genes for enzymes of the central metabolism. *J. Biotechnol.* **154**, 126–139.

Aung, H.L., Berney, M., and Cook, G.M. 2014. Hypoxia-activated cytochrome *bd* expression in *Mycobacterium smegmatis* is cyclic AMP receptor protein dependent. *J. Bacteriol.* **196**, 3091–3097.

Aung, H.L., Dixon, L.L., Smith, L.J., Sweeney, N.P., Robson, J.R., Berney, M., Buxton, R.S., Green, J., and Cook, G.M. 2015. Novel regulatory roles of cAMP receptor proteins in fast-growing environmental mycobacteria. *Microbiology* **161**, 648–661.

Beatty, C.M., Browning, D.F., Busby, S.J.W., and Wolfe, A.J. 2003. Cyclic AMP receptor protein-dependent activation of the *Escherichia coli acs*P2 promoter by a synergistic class III mechanism. *J. Bacteriol.* **185**, 5148–5157.

Berg, P. 1956. Acyl adenylates; an enzymatic mechanism of acetate activation. *J. Biol. Chem.* **222**, 991–1013.

Beste, D.J.V., Noh, K., Niedenfuhr, S., Mendum, T.A., Hawkins, N.D., Ward, J.L., Beale, M.H., Wiechert, W., and McFadden, J. 2013. 13C-flux spectral analysis of host-pathogen metabolism reveals a mixed diet for intracellular *Mycobacterium tuberculosis*. *Chem. Biol.* **20**, 1012–1021.

Bloch, H. and Segal, W. 1956. Biochemical differentiation of *Mycobacterium tuberculosis* grown *in vivo* and *in vitro*. *J. Bacteriol.* **72**, 132–141.

Bong, H.J., Ko, E.M., Song, S.Y., Ko, I.J., and Oh, J.I. 2019. Tripartite regulation of the *glpFKD* operon involved in glycerol catabolism by GylR, Crp, and SigF in *Mycobacterium smegmatis*. *J. Bacteriol.* **201**, e00511-19.

Brown, T.D., Jones-Mortimer, M.C., and Kornberg, H.L. 1977. The enzymic interconversion of acetate and acetyl-coenzyme A in *Escherichia coli*. *J. Gen. Microbiol.* **102**, 327–336.

Browning, D.F., Beatty, C.M., Sanstad, E.A., Gunn, K.E., Busby, S.J.W., and Wolfe, A.J. 2004. Modulation of CRP-dependent transcription at the *Escherichia coli acs*P2 promoter by nucleoprotein complexes: anti-activation by the nucleoid proteins FIS and IHF. *Mol. Microbiol.* **51**, 241–254.

Chopra, T., Hamelin, R., Armand, F., Chiappe, D., Moniatte, M., and McKinney, J.D. 2014. Quantitative mass spectrometry reveals plasticity of metabolic networks in *Mycobacterium smegmatis*. *Mol. Cell. Proteomics* **13**, 3014–3028.

Clark, D.P. and Cronan, J.E. 2005. Two-carbon compounds and fatty acids as carbon sources. *EcoSal Plus* **1**. doi: 10.1128/ecosalplus.3.4.4.

Cramer, A., Gerstmeir, R., Schaffer, S., Bott, M., and Eikmanns, B.J. 2006. Identification of RamA, a novel LuxR-type transcriptional regulator of genes involved in acetate metabolism of *Corynebacterium glutamicum*. *J. Bacteriol.* **188**, 2554–2567.

Crosby, H.A., Heiniger, E.K., Harwood, C.S., and Escalante-Semerena, J.C. 2010. Reversible *N*ε-lysine acetylation regulates the activity of acyl-CoA synthetases involved in anaerobic benzoate catabolism in *Rhodopseudomonas palustris*. *Mol. Microbiol.* **76**, 874–888.

Enjalbert, B., Millard, P., Dinclaux, M., Portais, J.C., and Létisse, F. 2017. Acetate fluxes in *Escherichia coli* are determined by the thermodynamic control of the Pta-AckA pathway. *Sci. Rep.* **7**, 42135.

Fox, D.K. and Roseman, S. 1986. Isolation and characterization of homogeneous acetate kinase from *Salmonella typhimurium* and *Escherichia coli*. *J. Biol. Chem.* **261**, 13487–13497.

Gardner, J.G. and Escalante-Semerena, J.C. 2009. In *Bacillus subtilis*, the sirtuin protein deacetylase, encoded by the *srtN* gene (formerly *yhdZ*), and functions encoded by the *acuABC* genes control the activity of acetyl coenzyme A synthetase. *J. Bacteriol.* **191**, 1749–1755.

Gardner, J.G., Grundy, F.J., Henkin, T.M., and Escalante-Semerena, J.C. 2006. Control of acetyl-coenzyme A synthetase (AcsA) activity by acetylation/deacetylation without NAD^+ involvement in *Bacillus subtilis*. *J. Bacteriol.* **188**, 5460–5468.

Gerstmeir, R., Cramer, A., Dangel, P., Schaffer, S., and Eikmanns, B.J. 2004. RamB, a novel transcriptional regulator of genes involved in acetate metabolism of *Corynebacterium glutamicum*. *J. Bacteriol.* **186**, 2798–2809.

Green, M.R. and Sambrook, J. 2012. Molrcular cloning: a laboratory manual, 4th edn. Cold Spring Harbor Laboratory Press, Cold Spring Harbor, New York, USA.

Green, J., Stapleton, M.R., Smith, L.J., Artymiuk, P.J., Kahramanoglou, C., Hunt, D.M., and Buxton, R.S. 2014. Cyclic-AMP and bacterial cyclic-AMP receptor proteins revisited: adaptation for different ecological niches. *Curr. Opin. Microbiol.* **18**, 1–7.

Grundy, F.J., Turinsky, A.J., and Henkin, T.M. 1994. Catabolite regulation of *Bacillus subtilis* acetate and acetoin utilization genes by CcpA. *J. Bacteriol.* **176**, 4527–4533.

Gu, J., Deng, J.Y., Li, R., Wei, H., Zhang, Z., Zhou, Y., Zhang, Y., and Zhang, X.E. 2009. Cloning and characterization of NAD-dependent protein deacetylase (Rv1151c) from *Mycobacterium tuberculosis*. *Biochemistry* **74**, 743–748.

Hayden, J.D., Brown, L.R., Gunawardena, H.P., Perkowski, E.F., Chen, X., and Braunstein, M. 2013. Reversible acetylation regulates acetate and propionate metabolism in *Mycobacterium smegmatis*. *Microbiology* **159**, 1986–1999.

Heroven, A.K. and Dersch, P. 2014. Coregulation of host-adapted metabolism and virulence by pathogenic yersiniae. *Front. Cell. Infect. Microbiol.* **4**, 146.

Jeong, J.A., Lee, H.N., Ko, I.J., and Oh, J.I. 2013. Development of new vector systems as genetic tools applicable to mycobacteria. *J. Life Sci.* **23**, 290–298.

Jeong, J.A., Park, S.W., Yoon, D., Kim, S., Kang, H.Y., and Oh, J.I. 2018. Roles of alanine dehydrogenase and induction of its gene in *Mycobacterium smegmatis* under respiration-inhibitory conditions. *J. Bacteriol.* **200**, e00152-18.

Jessee, J. 1986. New subcloning efficiency competent cells: > 1 × 106 transformants/mg. *Focus* **8**, 9–10.

Kakuda, H., Hosono, K., Shiroishi, K., and Ichihara, S. 1994. Identification and characterization of the *ackA* (acetate kinase A)-*pta* (phosphotransacetylase) operon and complementation analysis of acetate utilization by an *ackA-pta* deletion mutant of *Escherichia coli*. *J. Biochem.* **116**, 916–922.

Kim, M.J., Park, K.J., Ko, I.J., Kim, Y.M., and Oh, J.I. 2010. Different roles of DosS and DosT in the hypoxic adaptation of Mycobacteria. *J. Bacteriol.* **192**, 4868–4875.

Ko, E.M., Kim, J.Y., Lee, S., Kim, S., Hwang, J., and Oh, J.I. 2021. Regulation of the *icl1* gene encoding the major isocitrate lyase in *Mycobacterium smegmatis*. *J. Bacteriol.* **203**, e0040221.

Ko, E.M. and Oh, J.I. 2020. Induction of the *cydAB* operon encoding the *bd* quinol oxidase under respiration-inhibitory conditions by the major cAMP receptor protein MSMEG_6189 in *Mycobacterium smegmatis*. *Front. Microbiol.* **11**, 608624.

Kumari, S., Beatty, C.M., Browning, D.F., Busby, S.J., Simel, E.J.,

Hovel-Miner, G., and Wolfe, A.J. 2000. Regulation of acetyl coenzyme A synthetase in *Escherichia coli*. *J. Bacteriol.* **182**, 4173–4179.

Kumari, S., Tishel, R., Eisenbach, M., and Wolfe, A.J. 1995. Cloning, characterization, and functional expression of *acs*, the gene which encodes acetyl coenzyme A synthetase in *Escherichia coli*. *J. Bacteriol.* **177**, 2878–2886.

Kuprat, T., Johnsen, U., Ortjohann, M., and Schönheit, P. 2020. Acetate metabolism in archaea: characterization of an acetate transporter and of enzymes involved in acetate activation and gluconeogenesis in *Haloferax volcanii*. *Front. Microbiol.* **11**, 604926.

Lee, H.N., Ji, C.J., Lee, H.H., Park, J., Seo, Y.S., Lee, J.W., and Oh, J.I. 2018. Roles of three FurA paralogs in the regulation of genes pertaining to peroxide defense in *Mycobacterium smegmatis* mc2 155. *Mol. Microbiol.* **108**, 661–682.

Lee, H.J., Lang, P.T., Fortune, S.M., Sassetti, C.M., and Alber, T. 2012. Cyclic AMP regulation of protein lysine acetylation in *Mycobacterium tuberculosis*. *Nat. Struct. Mol. Biol.* **19**, 811–818.

Lee, H.N., Lee, N.O., Han, S.J., Ko, I.J., and Oh, J.I. 2014. Regulation of the *ahpC* gene encoding alkyl hydroperoxide reductase in *Mycobacterium smegmatis*. *PLoS ONE* **9**, e111680.

Lee, W., VanderVen, B.C., Fahey, R.J., and Russell, D.G. 2013. Intracellular *Mycobacterium tuberculosis* exploits host-derived fatty acids to limit metabolic stress. *J. Biol. Chem.* **288**, 6788–6800.

Li, R., Gu, J., Chen, P., Zhang, Z., Deng, J., and Zhang, X. 2011. Purification and characterization of the acetyl-CoA synthetase from *Mycobacterium tuberculosis*. *Acta Biochim. Biophys. Sin.* **43**, 891–899.

Liu, W.B., Liu, X.X., Shen, M.J., She, G.L., and Ye, B.C. 2019. The nitrogen regulator GlnR directly controls transcription of the *prpDBC* operon involved in methylcitrate cycle in *Mycobacterium smegmatis*. *J. Bacteriol.* **201**, e00099-19.

Liu, X.X., Shen, M.J., Liu, W.B., and Ye, B.C. 2018. GlnR-mediated regulation of short-chain fatty acid assimilation in *Mycobacterium smegmatis*. *Front. Microbiol.* **9**, 1311.

Masiewicz, P., Brzostek, A., Wolański, M., Dziadek, J., and Zakrzewska-Czerwińska, J. 2012. A novel role of the PrpR as a transcription factor involved in the regulation of methylcitrate pathway in *Mycobacterium tuberculosis*. *PLoS ONE* **7**, e43651.

Micklinghoff, J.C., Breitinger, K.J., Schmidt, M., Geffers, R., Eikmanns, B.J., and Bange, F.C. 2009. Role of the transcriptional regulator RamB (Rv0465c) in the control of the glyoxylate cycle in *Mycobacterium tuberculosis*. *J. Bacteriol.* **191**, 7260–7269.

Molle, V., Nakaura, Y., Shivers, R.P., Yamaguchi, H., Losick, R., Fujita, Y., and Sonenshein, A.L. 2003. Additional targets of the *Bacillus subtilis* global regulator CodY identified by chromatin immunoprecipitation and genome-wide transcript analysis. *J. Bacteriol.* **185**, 1911–1922.

Munoz-Elias, E.J. and McKinney, J.D. 2005. *Mycobacterium tuberculosis* isocitrate lyases 1 and 2 are jointly required for *in vivo* growth and virulence. *Nat. Med.* **11**, 638–644.

Nambi, S., Badireddy, S., Visweswariah, S.S., and Anand, G.S. 2012. Cyclic AMP-induced conformational changes in mycobacterial protein acetyltransferases. *J. Biol. Chem.* **287**, 18115–18129.

Nambi, S., Basu, N., and Visweswariah, S.S. 2010. cAMP-regulated protein lysine acetylases in mycobacteria. *J. Biol. Chem.* **285**, 24313–24323.

Nambi, S., Gupta, K., Bhattacharyya, M., Ramakrishnan, P., Ravikumar, V., Siddiqui, N., Thomas, A.T., and Visweswariah, S.S. 2013. Cyclic AMP-dependent protein lysine acylation in mycobacteria regulates fatty acid and propionate metabolism. *J. Biol. Chem.* **288**, 14114–14124.

Oh, J.I. and Kaplan, S. 1999. The *cbb3* terminal oxidase of *Rhodobacter sphaeroides* 2.4.1: structural and functional implications for the regulation of spectral complex formation. *Biochemistry* **38**, 2688–2696.

Pandey, A.K. and Sassetti, C.M. 2008. Mycobacterial persistence requires the utilization of host cholesterol. *Proc. Natl. Acad. Sci. USA* **105**, 4376–4380.

Puckett, S., Trujillo, C., Wang, Z., Eoh, H., Ioerger, T.R., Krieger, I., Sacchettini, J., Schnappinger, D., Rhee, K.Y., and Ehrt, S. 2017. Glyoxylate detoxification is an essential function of malate synthase required for carbon assimilation in *Mycobacterium tuberculosis*. *Proc. Natl. Acad. Sci. USA* **114**, E2225–E2232.

Qi, N., She, G.L., Du, W., and Ye, B.C. 2021. *Mycobacterium smegmatis* GlnR regulates the glyoxylate cycle and the methylcitrate cycle on fatty acid metabolism by repressing *icl* transcription. *Front. Microbiol.* **12**, 603835.

Reinscheid, D.J., Schnicke, S., Rittmann, D., Zahnow, U., Sahm, H., and Eikmanns, B.J. 1999. Cloning, sequence analysis, expression and inactivation of the *Corynebacterium glutamicum pta-ack* operon encoding phosphotransacetylase and acetate kinase. *Microbiology* **145**, 503–513.

Rickman, L., Scott, C., Hunt, D.M., Hutchinson, T., Menéndez, M.C., Whalan, R., Hinds, J., Colston, M.J., Green, J., and Buxton, R.S. 2005. A member of the cAMP receptor protein family of transcription regulators in *Mycobacterium tuberculosis* is required for virulence in mice and controls transcription of the *rpfA* gene coding for a resuscitation promoting factor. *Mol. Microbiol.* **56**, 1274–1286.

Robinson, M.D., McCarthy, D.J., and Smyth, G.K. 2010. edgeR: a Bioconductor package for differential expression analysis of digital gene expression data. *Bioinformatics* **26**, 139–140.

Rücker, N., Billig, S., Bücker, R., Jahn, D., Wittmann, C., and Bange, F.C. 2015. Acetate dissimilation and assimilation in *Mycobacterium tuberculosis* depend on carbon availability. *J. Bacteriol.* **197**, 3182–3190.

Sadykov, M.R., Thomas, V.C., Marshall, D.D., Wenstrom, C.J., Moormeier, D.E., Widhelm, T.J., Nuxoll, A.S., Powers, R., and Bayles, K.W. 2013. Inactivation of the Pta-AckA pathway causes cell death in *Staphylococcus aureus*. *J. Bacteriol.* **195**, 3035–3044.

Sharma, R., Zaveri, A., Gopalakrishnapai, J., Srinath, T., Varshney, U., and Visweswariah, S.S. 2014. Paralogous cAMP receptor proteins in *Mycobacterium smegmatis* show biochemical and functional divergence. *Biochemistry* **53**, 7765–7776.

Shimada, T., Fujita, N., Yamamoto, K., and Ishihama, A. 2011. Novel roles of cAMP receptor protein (CRP) in regulation of transport and metabolism of carbon sources. *PLoS ONE* **6**, e20081.

Shin, J.H., Yang, J.Y., Jeon, B.Y., Yoon, Y.J., Cho, S.N., Kang, Y.H., Ryu, D.H., and Hwang, G.S. 2011. 1H NMR-based metabolomic profiling in mice infected with *Mycobacterium tuberculosis*. *J. Proteome Res.* **10**, 2238–2247.

Snapper, S.B., Melton, R.E., Mustafa, S., Kieser, T., and Jacobs, W.R.Jr. 1990. Isolation and characterization of efficient plasmid transformation mutants of *Mycobacterium smegmatis*. *Mol. Microbiol.* **4**, 1911–1919.

Somashekar, B.S., Amin, A.G., Rithner, C.D., Troudt, J., Basaraba, R., Izzo, A., Crick, D.C., and Chatterjee, D. 2011. Metabolic profiling of lung granuloma in *Mycobacterium tuberculosis* infected guinea pigs: *ex vivo* 1H magic angle spinning NMR studies. *J. Proteome Res.* **10**, 4186–4195.

Starai, V.J., Celic, I., Cole, R.N., Boeke, J.D., and Escalante-Semerena, J.C. 2002. Sir2-dependent activation of acetyl-CoA synthetase by deacetylation of active lysine. *Science* **298**, 2390–2392.

Starai, V.J. and Escalante-Semerena, J.C. 2004. Identification of the protein acetyltransferase (Pat) enzyme that acetylates acetyl-CoA synthetase in *Salmonella enterica*. *J. Mol. Biol.* **340**, 1005–1012.

Stover, C.K., de la Cruz, V.F., Fuerst, T.R., Burlein, J.E., Benson, L.A., Bennett, L.T., Bansal, G.P., Young, J.F., Lee, M.H., Hatfull, G.F., *et al.* 1991. New use of BCG for recombinant vaccines. *Nature* **351**, 456–460.

Tabor, S. and Richardson, C.C. 1985. A bacteriophage T7 RNA polymerase/promoter system for controlled exclusive expression of specific genes. *Proc. Natl. Acad. Sci. USA* **82**, 1074–1078.

Utsumi, R., Noda, M., Kawamukai, M., and Komano, T. 1989. Control mechanism of the *Escherichia coli* K-12 cell cycle is triggered by the cyclic AMP-cyclic AMP receptor protein complex. *J. Bacteriol.* **171**, 2909–2912.

Van den Berg, M.A. and Steensma, H.Y. 1995. ACS2, a *Saccharomyces cerevisiae* gene encoding acetyl-coenzyme A synthetase, essential for growth on glucose. *Eur. J. Biochem.* **231**, 704–713.

VanderVen, B.C., Fahey, R.J., Lee, W., Liu, Y., Abramovitch, R.B., Memmott, C., Crowe, A.M., Eltis, L.D., Perola, E., Deininger, D.D., *et al.* 2015. Novel inhibitors of cholesterol degradation in *Mycobacterium tuberculosis* reveal how the bacterium's metabolism is constrained by the intracellular environment. *PLoS Pathog.* **11**, e1004679.

Webster, L.T.Jr. 1963. Studies of the acetyl coenzyme A synthetase reaction. I. Isolation and characterization of enzyme-bound acetyl adenylate. *J. Biol. Chem.* **238**, 4010–4015.

Wolfe, A.J. 2005. The acetate switch. *Microbiol. Mol. Biol. Rev.* **69**, 12–50.

Xu, H., Hegde, S.S., and Blanchard, J.S. 2011. Reversible acetylation and inactivation of *Mycobacterium tuberculosis* acetyl-CoA synthetase is dependent on cAMP. *Biochemistry* **50**, 5883–5892.

Xu, J.Y., Zhao, L., Liu, X., Hu, H., Liu, P., Tan, M., and Ye, B.C. 2018. Characterization of the lysine acylomes and the substrates regulated by protein acyltransferase in *Mycobacterium smegmatis*. *ACS Chem. Biol.* **13**, 1588–1597.

Yanisch-Perron, C., Vieira, J., and Messing, J. 1985. Improved M13 phage cloning vectors and host strains: nucleotide sequences of the M13mp18 and pUC19 vectors. *Gene* **33**, 103–119.

Yu, B.J., Kim, J.A., Moon, J.H., Ryu, S.E., and Pan, J.G. 2008. The diversity of lysine-acetylated proteins in *Escherichia coli*. *J. Microbiol. Biotechnol.* **18**, 1529–1536.

Zalieckas, J.M., Wray, L.V.Jr., and Fisher, S.H. 1998. Expression of the *Bacillus subtilis acsA* gene: position and sequence context affect cre-mediated carbon catabolite repression. *J. Bacteriol.* **180**, 6649–6654.